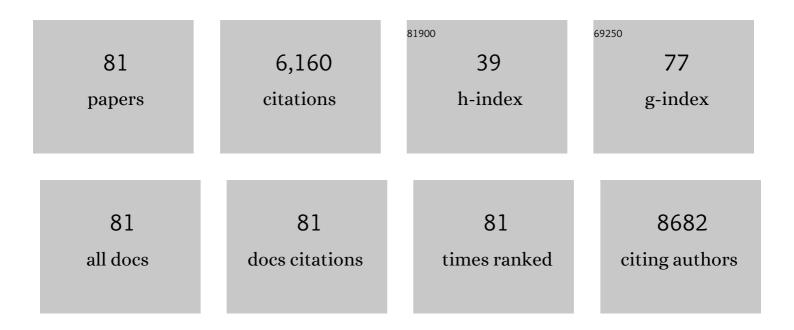
Xiaoqiang An

List of Publications by Year in descending order

Source: https://exaly.com/author-pdf/8943691/publications.pdf Version: 2024-02-01



#	Article	IF	CITATIONS
1	A critical review of CO2 photoconversion: Catalysts and reactors. Catalysis Today, 2014, 224, 3-12.	4.4	581
2	Graphene-based photocatalytic composites. RSC Advances, 2011, 1, 1426.	3.6	499
3	WO3 nanorods/graphene nanocomposites for high-efficiency visible-light-driven photocatalysis and NO2 gas sensing. Journal of Materials Chemistry, 2012, 22, 8525.	6.7	484
4	Cu ₂ O/Reduced Graphene Oxide Composites for the Photocatalytic Conversion of CO ₂ . ChemSusChem, 2014, 7, 1086-1093.	6.8	387
5	Cu ₂ ZnSnS ₄ -Pt and Cu ₂ ZnSnS ₄ -Au Heterostructured Nanoparticles for Photocatalytic Water Splitting and Pollutant Degradation. Journal of the American Chemical Society, 2014, 136, 9236-9239.	13.7	374
6	The synergetic effects of Ti ₃ C ₂ MXene and Pt as co-catalysts for highly efficient photocatalytic hydrogen evolution over g-C ₃ N ₄ . Physical Chemistry Chemical Physics, 2018, 20, 11405-11411.	2.8	189
7	Biomolecule-assisted self-assembly of CdS/MoS 2 /graphene hollow spheres as high-efficiency photocatalysts for hydrogen evolution without noble metals. Applied Catalysis B: Environmental, 2016, 182, 504-512.	20.2	175
8	Defect Modulation of Z-Scheme TiO ₂ /Cu ₂ O Photocatalysts for Durable Water Splitting. ACS Catalysis, 2019, 9, 8346-8354.	11.2	146
9	One-pot synthesis of In2S3 nanosheets/graphene composites with enhanced visible-light photocatalytic activity. Applied Catalysis B: Environmental, 2013, 129, 80-88.	20.2	145
10	Biomolecule-assisted fabrication of copper doped SnS ₂ nanosheet–reduced graphene oxide junctions with enhanced visible-light photocatalytic activity. Journal of Materials Chemistry A, 2014, 2, 1000-1005.	10.3	144
11	Recent advances on photocatalytic fuel cell for environmental applications—The marriage of photocatalysis and fuel cells. Science of the Total Environment, 2019, 668, 966-978.	8.0	144
12	A critical review of g-C3N4-based photocatalytic membrane for water purification. Chemical Engineering Journal, 2021, 412, 128663.	12.7	144
13	Microstructure of carbon nitride affecting synergetic photocatalytic activity: Hydrogen bonds vs. structural defects. Applied Catalysis B: Environmental, 2017, 204, 49-57.	20.2	143
14	Electroactive Modified Carbon Nanotube Filter for Simultaneous Detoxification and Sequestration of Sb(III). Environmental Science & Technology, 2019, 53, 1527-1535.	10.0	111
15	CdS nanorods/reduced graphene oxide nanocomposites for photocatalysis and electrochemical sensing. Journal of Materials Chemistry A, 2013, 1, 5158.	10.3	101
16	New Insights into Defectâ€Mediated Heterostructures for Photoelectrochemical Water Splitting. Advanced Energy Materials, 2016, 6, 1502268.	19.5	95
17	Polyoxometalates/TiO2 Fenton-like photocatalysts with rearranged oxygen vacancies for enhanced synergetic degradation. Applied Catalysis B: Environmental, 2019, 244, 407-413.	20.2	92
18	Multi-electric field modulation for photocatalytic oxygen evolution: Enhanced charge separation by coupling oxygen vacancies with faceted heterostructures. Nano Energy, 2018, 51, 764-773.	16.0	88

#	Article	IF	CITATIONS
19	Polyoxometalates/TiO2 photocatalysts with engineered facets for enhanced degradation of bisphenol A through persulfate activation. Applied Catalysis B: Environmental, 2020, 268, 118394.	20.2	88
20	Hierarchical Nanotubular Anatase/Rutile/TiO ₂ (B) Heterophase Junction with Oxygen Vacancies for Enhanced Photocatalytic H ₂ Production. Langmuir, 2018, 34, 1883-1889.	3.5	85
21	Oxygen vacancy mediated construction of anatase/brookite heterophase junctions for high-efficiency photocatalytic hydrogen evolution. Journal of Materials Chemistry A, 2017, 5, 24989-24994.	10.3	81
22	Hydrogen-Bond-Mediated Self-Assembly of Carbon-Nitride-Based Photo-Fenton-like Membranes for Wastewater Treatment. Environmental Science & Technology, 2019, 53, 6981-6988.	10.0	79
23	Enhanced magnetic and optical properties of pure and (Mn, Sr) doped BiFeO3 nanocrystals. Solid State Communications, 2009, 149, 711-714.	1.9	77
24	The effect of the Ga content on the photocatalytic hydrogen evolution of Culn _{1â^'x} Ga _x S ₂ nanocrystals. Journal of Materials Chemistry A, 2014, 2, 12317.	10.3	76
25	Efficient conversion of dimethylarsinate into arsenic and its simultaneous adsorption removal over FeCx/N-doped carbon fiber composite in an electro-Fenton process. Water Research, 2016, 100, 57-64.	11.3	71
26	ZnO@ZnS hollow dumbbells–graphene composites as high-performance photocatalysts and alcohol sensors. New Journal of Chemistry, 2012, 36, 2593.	2.8	67
27	Boosting photoelectrochemical activities of heterostructured photoanodes through interfacial modulation of oxygen vacancies. Nano Energy, 2017, 35, 290-298.	16.0	59
28	Dual channel construction of WO3 photocatalysts by solution plasma for the persulfate-enhanced photodegradation of bisphenol A. Applied Catalysis B: Environmental, 2020, 277, 119221.	20.2	56
29	Interfacial charge separation in Cu ₂ O/RuO _x as a visible light driven CO ₂ reduction catalyst. Physical Chemistry Chemical Physics, 2014, 16, 5922-5926.	2.8	55
30	3-D hierarchical Ag/ZnO@CF for synergistically removing phenol and Cr(VI): Heterogeneous vs. homogeneous photocatalysis. Journal of Colloid and Interface Science, 2020, 558, 85-94.	9.4	55
31	Effect of Single-Atom Cocatalysts on the Activity of Faceted TiO ₂ Photocatalysts. Langmuir, 2019, 35, 391-397.	3.5	54
32	Emerging graphitic carbon nitride-based membranes for water purification. Water Research, 2021, 200, 117207.	11.3	53
33	Synergistic effect of dual sites on bimetal-organic frameworks for highly efficient peroxide activation. Journal of Hazardous Materials, 2021, 406, 124692.	12.4	52
34	Strongly Coupled Metal Oxide/Reassembled Carbon Nitride/Co–Pi Heterostructures for Efficient Photoelectrochemical Water Splitting. ACS Applied Materials & Interfaces, 2018, 10, 6424-6432.	8.0	50
35	Intercalation of Nanosized Fe ₃ C in Iron/Carbon To Construct Multifunctional Interface with Reduction, Catalysis, Corrosion Resistance, and Immobilization Capabilities. ACS Applied Materials & Interfaces, 2019, 11, 15709-15717.	8.0	50
36	Insight into the Key Role of Cr Intermediates in the Efficient and Simultaneous Degradation of Organic Contaminants and Cr(VI) Reduction via g-C ₃ N ₄ -Assisted Photocatalysis. Environmental Science & Technology, 2022, 56, 3552-3563.	10.0	48

#	Article	IF	CITATIONS
37	Facet-Regulating Local Coordination of Dual-Atom Cocatalyzed TiO ₂ for Photocatalytic Water Splitting. ACS Catalysis, 2021, 11, 14669-14676.	11.2	42
38	Growth and Field Emission Properties of Cactus-like Gallium Oxide Nanostructures. Journal of Physical Chemistry C, 2008, 112, 95-98.	3.1	41
39	Assembly-synthesis of puff pastry-like g-C3N4/CdS heterostructure as S-junctions for efficient photocatalytic water splitting. Chemical Engineering Journal, 2022, 431, 133348.	12.7	41
40	Enhanced Electroreductive Removal of Bromate by a Supported Pd–In Bimetallic Catalyst: Kinetics and Mechanism Investigation. Environmental Science & Technology, 2016, 50, 11872-11878.	10.0	39
41	Decomplexation of Cu(II)-EDTA over oxygen-doped g-C3N4: An available resource towards environmental sustainability. Chemical Engineering Journal, 2018, 345, 138-146.	12.7	35
42	Controllable hydrothermal synthesis of Cu2S nanowires on the copper substrate. Materials Letters, 2010, 64, 252-254.	2.6	34
43	Strongly coupled polyoxometalates/oxygen doped g-C3N4 nanocomposites as Fenton-like catalysts for efficient photodegradation of sulfosalicylic acid. Catalysis Communications, 2018, 112, 63-67.	3.3	34
44	Facet-dependent activity of TiO2/covalent organic framework S-scheme heterostructures for CO2 photoreduction. Chemical Engineering Journal, 2022, 442, 135279.	12.7	34
45	Exfoliation method matters: The microstructure-dependent photoactivity of g-C3N4 nanosheets for water purification. Journal of Hazardous Materials, 2022, 424, 127424.	12.4	32
46	Faceted TiO2 photocatalytic degradation of anthraquinone in aquatic solution under solar irradiation. Science of the Total Environment, 2019, 688, 592-599.	8.0	29
47	Microfluidic-enhanced 3-D photoanodes with free interfacial energy barrier for photoelectrochemical applications. Applied Catalysis B: Environmental, 2019, 244, 740-747.	20.2	29
48	Interface-modulated nanojunction and microfluidic platform for photoelectrocatalytic chemicals upgrading. Applied Catalysis B: Environmental, 2021, 282, 119541.	20.2	29
49	One-step exfoliation of polymeric C3N4 by atmospheric oxygen doping for photocatalytic persulfate activation. Journal of Colloid and Interface Science, 2020, 579, 455-462.	9.4	28
50	Efficient design principle for interfacial charge separation in hydrogen-intercalated nonstoichiometric oxides. Nano Energy, 2018, 53, 887-897.	16.0	27
51	New insights into interfacial photocharge transfer in TiO ₂ /C ₃ N ₄ heterostructures: effects of facets and defects. New Journal of Chemistry, 2019, 43, 4511-4517.	2.8	27
52	Defect modulation of MOF-derived ZnFe2O4/CNTs microcages for persulfate activation: Enhanced nonradical catalytic oxidation. Chemical Engineering Journal, 2022, 431, 133369.	12.7	27
53	A dual-biomimetic photocatalytic fuel cell for efficient electricity generation from degradation of refractory organic pollutants. Applied Catalysis B: Environmental, 2021, 298, 120501.	20.2	26
54	New insights into the surface-dependent activity of graphitic felts for the electro-generation of H2O2. Applied Surface Science, 2020, 509, 144875.	6.1	25

#	Article	IF	CITATIONS
55	Defect-enhanced activation of carbon nitride/horseradish peroxidase nanohybrids for visible-light-driven photobiocatalytic water purification. Chemical Engineering Journal, 2021, 408, 127231.	12.7	25
56	Coeffect of Silk Fibroin and Self-Assembly Monolayers on the Biomineralization of Calcium Carbonate. Journal of Physical Chemistry C, 2008, 112, 15844-15849.	3.1	23
57	Visualizing the Interfacial Charge Transfer between Photoactive <i>Microcystis aeruginosa</i> and Hydrogenated TiO ₂ . Environmental Science & Technology, 2020, 54, 10323-10332.	10.0	21
58	Biomineralization of CaCO ₃ through the Cooperative Interactions between Multiple Additives and Self-Assembled Monolayers. Journal of Physical Chemistry C, 2008, 112, 6526-6530.	3.1	20
59	Facet-dependent intermediate formation and reaction mechanism of photocatalytic removing hydrophobic anthracene under simulated solar irradiation. Applied Catalysis B: Environmental, 2017, 206, 194-202.	20.2	19
60	Bifunctional Photoelectrode Driven by Charged Domain Walls in Ferroelectric Bi ₂ WO ₆ . ACS Applied Energy Materials, 2020, 3, 4149-4154.	5.1	19
61	Synergy of cyano groups and cobalt single atoms in graphitic carbon nitride for enhanced bio-denitrification. Water Research, 2022, 218, 118465.	11.3	19
62	Light absorption modulation of novel Fe ₂ TiO ₅ inverse opals for photoelectrochemical water splitting. New Journal of Chemistry, 2017, 41, 7966-7971.	2.8	18
63	Synergetic Photocatalytic Pure Water Splitting and Self-Supplied Oxygen Activation by 2-D WO ₃ /TiO ₂ Heterostructures. ACS Sustainable Chemistry and Engineering, 2019, 7, 19902-19909.	6.7	18
64	Interfacial Charge Transfer in MoS2/TiO2 Heterostructured Photocatalysts: The Impact of Crystal Facets and Defects. Molecules, 2019, 24, 1769.	3.8	18
65	g-C3N4 nanofibers network reinforced polyamide nanofiltration membrane for fast desalination. Separation and Purification Technology, 2022, 293, 121125.	7.9	18
66	Largeâ€Area Printing of Ferroelectric Surface and Superâ€Domain for Solar Water Splitting. Advanced Functional Materials, 2022, 32, .	14.9	17
67	Bio-inspired fabrication of ZnO nanorod arrays and their optical and photoresponse properties. Journal of Crystal Growth, 2007, 308, 340-347.	1.5	16
68	Revealing Surface Charge Population on Flake-Like BiVO ₄ Photocatalysts by Single Particle Imaging Spectroscopies. ACS Applied Energy Materials, 2021, 4, 2543-2551.	5.1	16
69	Colloidal synthesis of SnS nanocrystals with dimension-dependent photoelectrochemical properties. New Journal of Chemistry, 2019, 43, 7457-7462.	2.8	15
70	Defect-enhanced photocatalytic removal of dimethylarsinic acid over mixed-phase mesoporous TiO2. Journal of Environmental Sciences, 2020, 91, 35-42.	6.1	15
71	Mo,Fe-codoped metal phosphide nanosheets derived from Prussian blue analogues for efficient overall water splitting. Journal of Colloid and Interface Science, 2022, 615, 456-464.	9.4	15
72	Oxygen vacancy modulation of {010}-dominated TiO2 for enhanced photodegradation of Sulfamethoxazole. Catalysis Communications, 2019, 118, 35-38.	3.3	13

#	Article	IF	CITATIONS
73	A strategy of enhancing photoactivity of TiO2 via facet-dependent pyrolysis of dicyandiamide. Applied Catalysis B: Environmental, 2020, 264, 118527.	20.2	10
74	Controllable Ferroelastic Switching in Epitaxial Self-Assembled Aurivillius Nanobricks. ACS Applied Materials & Interfaces, 2019, 11, 7296-7302.	8.0	9
75	Water-plasma-activated g-C3N4 for enhanced photodegradation of bisphenol A synergized with persulfate oxidation. Applied Surface Science, 2022, 592, 153163.	6.1	9
76	A promising treatment method for Cr(VI) detoxification and recovery by coupling Fe0/Fe3C/C fine powders and circulating fluidized bed. Chemical Engineering Journal, 2020, 398, 125565.	12.7	8
77	Silvered TiO2 for Facet-Dependent Photocatalytic Denitrification. ACS Applied Nano Materials, 0, , .	5.0	7
78	Optical and photocatalytic properties of sulfide semiconductor quantum dots (QDs) synthesized by silk fibroin template. Materials Letters, 2008, 62, 2754-2757.	2.6	6
79	Fabrication of Biocompatible Zn–Cysteine Nanowires and Their Application in Selective Fluorescence Detection of Cu ²⁺ . Journal of Nanoscience and Nanotechnology, 2010, 10, 8356-8361.	0.9	4
80	Characterization on the formation mechanism of Fe0/Fe3C/C nanostructure and its effect on PMS activation performance towards BPA degradation. Chemical Engineering Journal, 2022, 435, 134709.	12.7	3
81	Synthesis of aligned ripple-like and helical structure silica fibres. Journal of Non-Crystalline Solids, 2007, 353, 1041-1045.	3.1	2